Kinetic and Thermomechanical Analysis of Hydrophobic–Hydrophilic Copolymer Thermosets Synthesized via Free-Radical Polymerization

M. Aflal M. Rahmathullah, Yossef A. Elabd, Giuseppe R. Palmese

Department of Chemical and Biological Engineering, Drexel University, Philadelphia, Pennsylvania 19104

ABSTRACT: The synthesis of a crosslinked copolymer of hydrophobic and hydrophilic monomers, diglycidyl ether of bisphenol A vinyl ester (VE), and 2-acrylamido 2-methyl 1-propane sulfonic acid (AMPS) respectively, is discussed. A methodology for real-time monitoring of the copolymerization reaction using transmission mode near infrared (NIR) spectroscopy was employed that resolves overlapping peaks associated with the reactive double bonds. The influence of solvent, monomer ratio, and initiator concentration on the kinetic behavior of the system was investigated. The method of Mayo and Lewis was used to provide a qualitative understanding of the microstructure being formed. At low conversions (<15%) and within the compositions of interest, greater VE homopolymerization as compared with AMPS homopolymerization was observed and the product of the reactivity ratios ($r_{AMPS} \cdot r_{VE}$) was close to 0.5, suggesting the formation of a moderately random copolymer structure. Thermo-mechanical analysis shows large concentrations of AMPS had a plasticizing effect on the network structure. Solvent removal using supercritical carbon dioxide and thermal drying were compared, and the drying technique were shown to have an effect on the glass transition temperature (T_g), with the lowest T_g being 146°C for supercritically dried samples and 121°C for thermally dried systems. Gel permeation chromatography shows that there is a significant fraction of an unbound mobile phase within the network structure that might be acting as a plasticizing agent for the copolymer structure. © 2009 Wiley Periodicals, Inc. J Appl Polym Sci 115: 1419–1427, 2010

Key words: copolymerization; glass transition temperature; thermosets

INTRODUCTION

A major research thrust has been the design of polymeric materials combining mechanical strength with functionality such as electrical responsiveness,[1] optical switching capabilities,[2] or ionic conductivity[3] for a number of applications.[4,5] Mechanically strong polymers are generally hydrophobic, whereas "functional" polymers are hydrophilic,[6] causing challenges associated with the controlled combination of such dissimilar materials. Several approaches for generating combinations of these materials have been realized, such as the use of surfactants,[6] irradiation techniques,[7,8] polymer blends,[9] synthesis of polymeric systems with comb-type or dendrimer-type geometries,[10,11] or block copolymers.[12] Specific control over the balance between hydrophobicity and hydrophilicity in polymer systems translates into control over the desired microstructure and material properties and numerous polymerization schemes may be utilized for this purpose.[13] Conventional free radical copolymerization is a well-established technique for which a diverse group of monomers have been studied,[13,14] where comonomer reactivities are strongly influenced by steric and electronic effects. Most of the work so far combining hydrophobic and hydrophilic monomers have been developed for the synthesis of graft copolymers[15] or linear copolymers.[16] Preparation of crosslinked networks combining hydrophobic and hydrophilic monomers has typically been carried out using embedded[17] or interpenetrating networks,[18] or grafting of hydrophilic groups onto thermosets.[19] There are few reports on the copolymerization of crosslinked hydrophobic and hydrophilic monomers,[20] and it is of interest to investigate such combinations to ascertain the possibility of preparing membranes which are mechanically robust and hydrophilic.

The material system of interest here combines the hydrophobic difunctional vinyl ester (VE) (dimethacrylate of diglycidyl ether of bisphenol A [DGEBA]) with a hydrophilic monofunctional comonomer, 2-acrylamido 2-methyl-1-propane sulfonic acid

(AMPS). This combination of monomers in *N,N*-dimethyl formamide (DMF) as a common diluent forms a crosslinked network. The VE serves as the crosslinking portion of the polymer that results in thermal and mechanical stability,[21] whereas AMPS acts both as a chain extender and an ion-conducting pathway within the crosslinked network.[3,19]

A unique method to determine copolymerization kinetics based on near infrared (NIR) spectroscopy (8000–4000 cm^{-1}) has also been developed. Significant work has been done in evaluating free radical polymerization kinetics using a variety of techniques such as calorimetry,[22] infrared spectroscopy, NMR spectroscopy,[23] and fluorescence probe methods.[24] Calorimetric techniques provide an evaluation of overall reaction kinetics and not individual monomer reaction rates, whereas mid-infrared spectroscopy has sample preparation difficulties associated with using a solvent at elevated temperatures.[25] Monitoring of polymerization reactions using NIR spectroscopy has been widely used,[26–28] although there are very few reports discussing the difficulties associated with resolving peak overlap between acrylate and methacrylate peaks in chain copolymerizations,[25,29] which typically requires the need for peak deconvolution. The method discussed here for monitoring such reactive groups on both comonomers suggests a facile technique to monitor individual monomer reaction rates. An understanding of the structure being formed is necessary to validate the presence of networks with well-dispersed comonomers. The polymerization kinetics evaluated using NIR spectroscopy was employed to elucidate the type of copolymer structure being formed from a terminal reaction model, using the linearization method of Mayo and Lewis.[13,30] This analysis has been used by numerous researchers for copolymerizations in systems such as VE/styrene,[31] maleic anhydride/norbornene,[32] or acrylonitrile/methyl acrlyate[33] using real-time NIR spectroscopy. The determined structure was linked to properties through thermo-mechanical analysis to show significant differences based on the initial comonomer ratios, and the technique used to remove DMF, i.e., either by thermal drying or by the use of supercritical carbon dioxide.[34]

The objectives of this work are: (i) to report the synthetic protocol for these new crosslinked copolymer system comprised of VE and AMPS (ii) to present and validate a method for accurately monitoring the copolymerization kinetics of this system using NIR spectroscopy, (iii) to evaluate the effects of various processing parameters, and (iv) to qualitatively postulate network structures being formed based on the values of reactivity ratios obtained from kinetic analyses and thermo-mechanical characterization.

EXPERIMENTAL

Materials

Difunctional VE resin was prepared as discussed previously[35] via a catalyzed methacrylation of 4,4'-diglycidyl ether of bisphenol A (DGEBA) (EPON 828, Miller Stephenson). Monofunctional 2-acrylamido 2-methyl 1-propane sulfonic acid (AMPS, 99%, Sigma Aldrich) was used as obtained. *N,N*-dimethyl formamide (DMF, 98%, Sigma Aldrich) and benzoyl peroxide (BPO, 99%, Sigma Aldrich) were also used as obtained. Figure 1 shows the chemical structures of the monomers and solvent used.

Synthesis

Varying molar ratios of VE to AMPS were prepared in DMF at known solvent weight fractions. The initiator concentration was fixed at either 0.02 or 0.002 mole fraction of BPO to vinyl groups present in the mixture. All reaction mixtures were typically prepared in 20 mL glass scintillation vials, and BPO was added only after complete dissolution of monomers in DMF. The reactant mixtures were immediately transferred into ampoules of fixed internal diameter and wall thickness (1.60 ± 0.05 mm). These ampoules were then hermetically sealed.

Spectroscopic analysis

Fourier transform infrared analysis was performed using a Nicolet Nexus 670 Spectrometer in the range of 4000–8000 cm^{-1} using a DTGS detector at an aperture setting of 100. The resolution was set at 8 cm^{-1}, and 32 scans were taken per spectrum. The sealed ampules were placed in a custom built sample holder equilibrated at 60°C as discussed in previous work.[36] Spectra were collected every 120 seconds until complete conversion was ascertained by the disappearance of the vinyl peak.
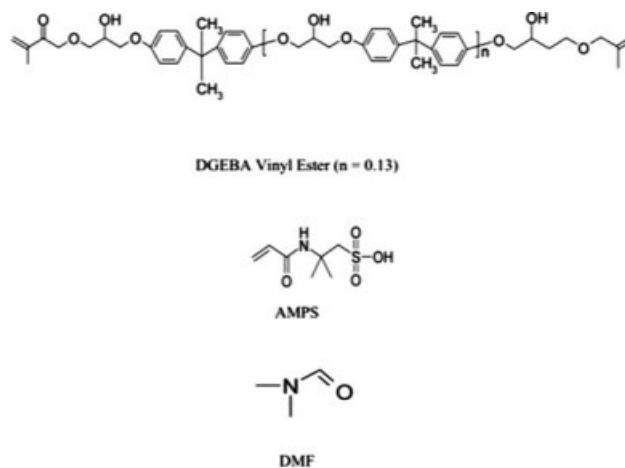

DGEBA Vinyl Ester (n = 0.13)

AMPS

DMF

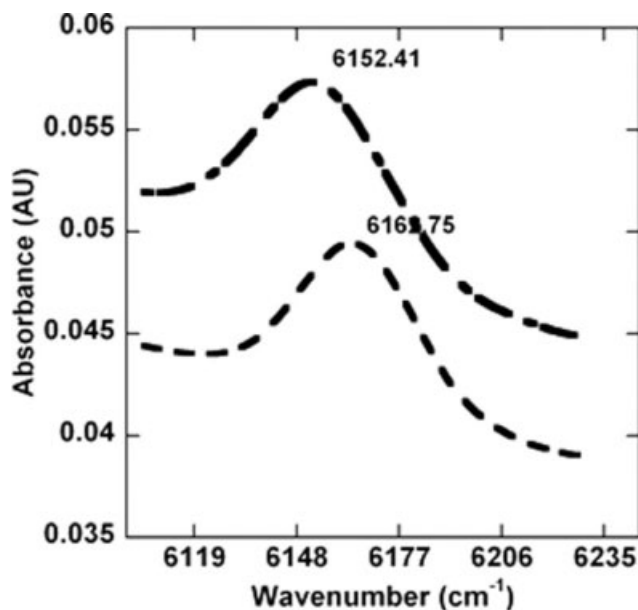**Figure 1** Chemical structure of reagents used.

Figure 2 Representative plot of near-IR absorbances of (–) pure VE and (- -) pure AMPS at a solvent fraction of 71.5 wt %.

Figure 2 shows the characteristic acrylate C=C peak at ~6152 cm^{-1} for pure AMPS (subscript 1) and the characteristic methacrylate C—C peak at ~6163 cm^{-1} associated with pure VE (subscript 2) at a 71.5 wt % solvent fraction. Spectra of mixtures of the unreacted monomers show a resultant peak position lying between these two limits. Figure 3 shows the resultant peak position at different times during the reaction and also indicates that the reaction appears to be going to completion. Table I reports the peak position at a representative solvent fraction for varying comonomer ratios, which shows a direct relationship between monomer ratio and peak position. It should be noted that the second decimal place was a reproducible number for a calibrated
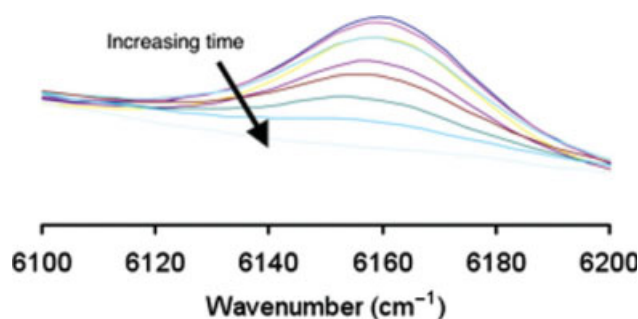

Figure 3 Representative IR spectra at VE : AMPS molar ratio of 2 : 3 at a 71.5 solvent (DMF) wt % indicating the decrease in peak area and shift in peak position as reaction proceeds with time. The spectra shown is between $t = 12$ min and $t = 1000$ min; at which time the reaction is apparently complete. [Color figure can be viewed in the online issue, which is available at www.interscience.wiley.com.]

TABLE I
Dependence of Peak Position on Molar Concentration of AMPS at a Fixed Solvent Content

AMPS (mol %)	Solvent content (wt %)	Peak position (cm^{-1})
0	71.5	6162.75
33	71.5	6161.26
50	71.5	6160.42
100	71.5	6152.41

sample setup. In analyzing this peak information two independent parameters are of interest. First, the peak position was a function of the molar ratio of VE to AMPS. Second, the peak area was directly dependent on the total C=C bond concentration as per Beer's Law:

$$A = \varepsilon c l \quad (1)$$

where A = absorbance (AU), ε = molar absorptivity (L mol^{-1} cm^{-1}), l = path length (cm) and c = concentration (mol L^{-1}). Assuming linear additivity[37] of the absorbances of VE and AMPS, the total peak area was solely a function of the total concentration of C=C bonds present in the system defined as

$$A_t = \varepsilon_1 c_1 l_1 + \varepsilon_2 c_2 l_2 \quad (2)$$

where A_t is the total absorbance due to both the monomers. Equation (2) reduces to Eq. (3) when l is constant between experiments and $\varepsilon' = \varepsilon l$.

$$A_t = \varepsilon_1' c_1 + \varepsilon_2' c_2 \quad (3)$$

Figure 4 shows the absorbance for AMPS in DMF and VE in DMF at different concentrations. From Beer's Law (**1**), the molar absorptivity is determined from the slope of a plot of absorbance versus concentration. These were found to be $\varepsilon_2' = 0.28$ L mol^{-1} (for VE) and $\varepsilon_1' = 0.281$ L mol^{-1} (AMPS).

Plots of the ratio between the molar concentration of VE (c_2) to AMPS (c_1), i.e., c_1/c_2 versus peak position were fitted to a second-order equation (Fig. 5) at a given solvent content. Individual plots for reactions in different solvent contents were used as there is a very slight dependence of peak position on solvent content. The fitted equation gives this molar ratio c_1/c_2 at any instant during the reaction as a function of peak position and was taken to be valid throughout the course of the reaction. At every instant at which c_1/c_2 was obtained, the peak area was recorded to give the total concentration of unreacted acrylate and methacrylate C=C present.

From the peak position and peak area obtained during the course of the reaction, individual values of c_1 and c_2 were determined using eqs. (4)–(6).
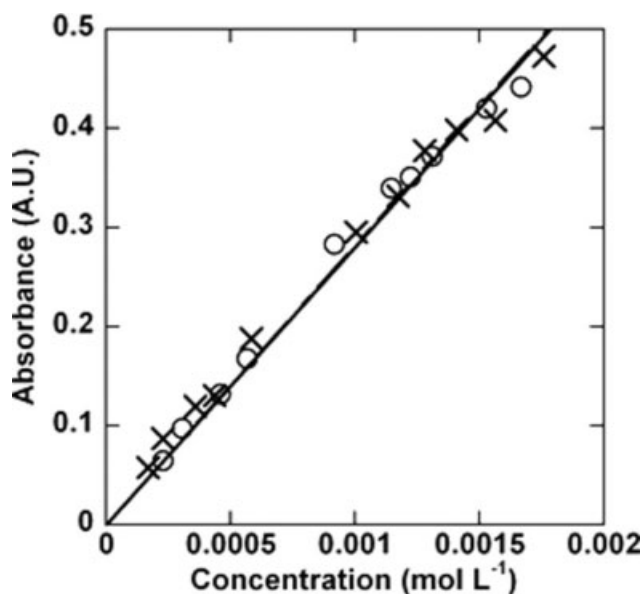
Figure 4 Plots of absorbance versus concentration of (O) VE and (X) AMPS at various molar concentrations of C=C bonds within the reactant mixture. The pure component molar absorptivity is taken as the slope of fitted line.

Defining α as

$$\alpha = \frac{c_1}{c_2} \quad (4)$$

and solving eqs. (3) and (4) results in:

$$c_2 = \frac{A_t}{(\varepsilon_1' \alpha + \varepsilon_2')} \quad (5)$$

The following are reasonable assumptions made in this analysis: (i) The molar absorptivities of VE and AMPS were independent of each other.[38] (ii) Peak interference due to the presence of DMF was negligible at all times. (iii) The ratio c_1/c_2 calculated using peak positions can be computed at all instances based on the calibration curve obtained at initial times. (iv) The minor dependence of peak position on solvent content does not appreciably affect the computation of fractional conversion.

Supercritical drying, dynamic mechanical analysis, and gel permeation chromatography

Samples for thermo-mechanical testing were prepared as follows. An assembly consisting of microscope glass slides separated by thin (~500 μm) Teflon® sheets held together with Teflon® tape were immersed in monomer solutions. Sealed containers of these were then cured at 60°C to completion (as determined by NIR spectroscopy). Samples were dried using supercritical carbon dioxide as detailed in previous work.[34] Viscoelastic behavior of the syn-

thesized copolymers was evaluated using a TA Instruments 2980 DMA in film tension geometry on rectangular samples that were cut down to premeasured sizes. The glass transition temperature, T_g was determined as the Tan δ maximum of the third temperature ramp taken at frequency of 1 Hz and a deflection of 5 μm, with a preload force of 0.01 N. The temperature ramp on the third run was between 35 and 250°C at a rate of 2°C/min. The first two temperature ramps were taken up to 200°C at a rate of 5 and 2°C/min, respectively, to remove the solvent.

Following cure, the extractable fraction might contain species other than the DMF used for the synthesis of the gels. Analysis of this fraction can shed light on the nature of this phase. This soluble portion was extracted by immersing a measured quantity of the crosslinked polymer (both critically dried and wet gels) in THF at a concentration of 2 mg of polymer/g of THF. This solution was passed through a 0.45 μm Nalgene® syringe filter and the extract used for analysis. Gel permeation chromatography (GPC) was carried out on these extracts using a Waters® 515 GPC with two 30 cm long, 7.5 mm diameter, 5 μm styrene-divinyl benzene columns in series. The columns were equilibrated and run at 30°C using THF as an eluent at a flow rate of 1 mL/min. The effluent was monitored using a Waters® 2487 UV detector set at 254 nm for the detection of phenyl groups. Since AMPS and large crosslinked species will not dissolve in THF, the extract from the polymer-solvent mixture should essentially be a measure of the presence of unattached high molecular weight molecules and unreacted VE, if any.
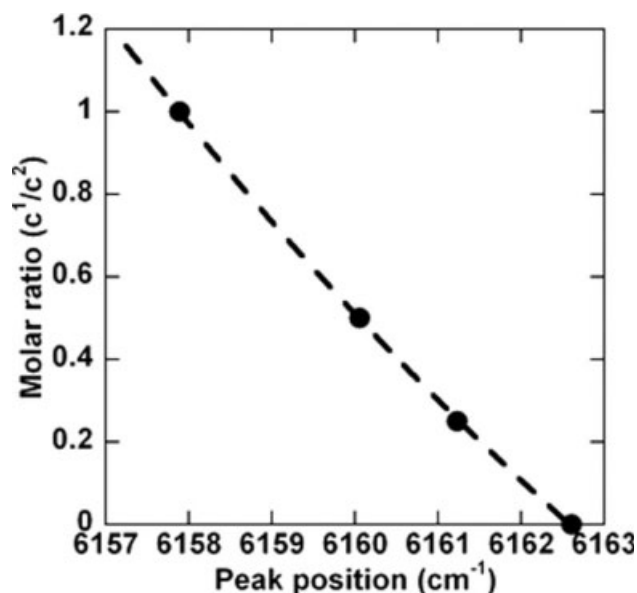

Figure 5 Representative calibration plot of comonomer molar ratio versus peak position at 75 wt % solvent fraction with a second order curve fit.
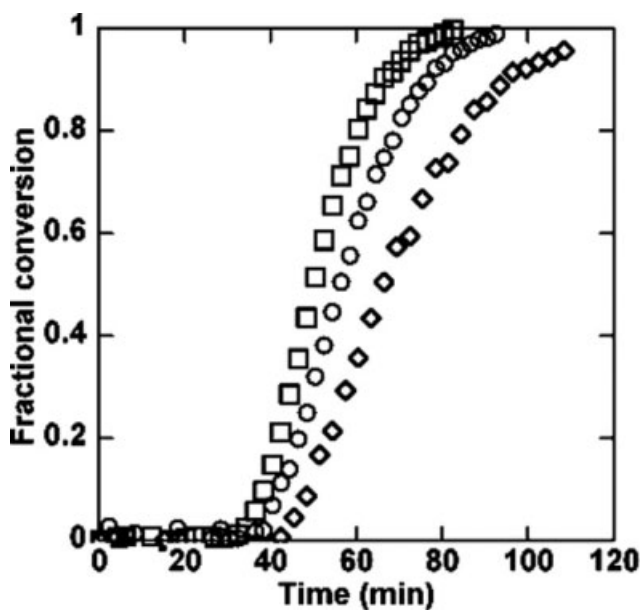
Figure 6 Temporal profile of fractional conversion in the homopolymerization of VE in DMF at (□) 33 wt %, (○) 25 wt % and (◇) 20 wt % VE in DMF.

RESULTS AND DISCUSSION

Cure behavior in VE-AMPS copolymers

Variations in comonomer ratios, solvent fractions, or initiator concentrations affects cure behavior and the resultant network structure. To study the homopolymerization of VE, pure VE monomer was dissolved in DMF at 33, 25, and 20 wt % VE in DMF with a BPO concentration of 0.02 molar fraction of vinyl groups. Figure 6 shows temporal conversion profiles for the three monomer concentrations. Spectroscopic data was analyzed using the method described in the experimental section for copolymerizing systems. The data show that inhibition times increase with increasing solvent concentrations. Moreover, the first order reaction rate constants as computed by taking the slope of the reaction profile are found to be 0.032, 0.026, and 0.019 sec^{-1} for the 33, 25, and 20 wt % VE in DMF, respectively. This change in reaction rates at varying degrees of dissolution suggests differences in the rates of diffusion-controlled termination and the subsequent autoacceleration. This trend is in agreement with the work of other researchers,[39] where termination via segmental rearrangement of radical chain ends lower reaction rates due to the decrease in diffusion limitations. Analysis of the spectral data showed no shift in peak. This is expected and lends support to our assertion that peak position shifts as a result of the presence of AMPS as a comonomer.

The influence of initiator concentration on reactivity was evaluated by keeping the molar ratio of VE : AMPS constant at 1 : 2 at a solvent content of 80 wt %. The initiator concentration was either 0.02 and 0.002 mol fraction of vinyl groups. Figure 7 shows temporal conversion profiles for both these compositions. As expected a significant increase in reactivity of the VE and AMPS was observed at higher initiator concentration. This increase is due to the increase in the number of polymer chain ends initiated.

Reaction mixtures with solvent weight fractions of 71.5 and 80 wt % DMF at a 1 : 2 VE : AMPS molar ratio were compared with evaluate the influence of solvent fraction on reactivity, Figure 8 shows temporal conversion profiles for these experiments. A distinct influence of solvent content on the onset of the Trommsdorf effect in both the VE and the AMPS was observed with the onset occurring earlier and at lower conversion for lower solvent content. It is also apparent that the increase in reactivity at the onset of autoacceleration is higher for the AMPS moieties when compared with VE. This suggests differences in the rates of termination and propagation of active species due to diffusion limitations resulting from network growth. The plots show that both the monomers continue reacting in such solvent-loaded systems apparently until complete conversion. This is in contrast to systems where a solvent is not present. For example in VE-Styrene systems, only styrene continues reacting after a certain point while the VE double bonds trapped in microgel structures do not.[40]

The addition of a comonomer affects the reaction rates of the VE and influences final material properties. Increasing the AMPS fraction yields softer materials. To evaluate a subset of materials for which
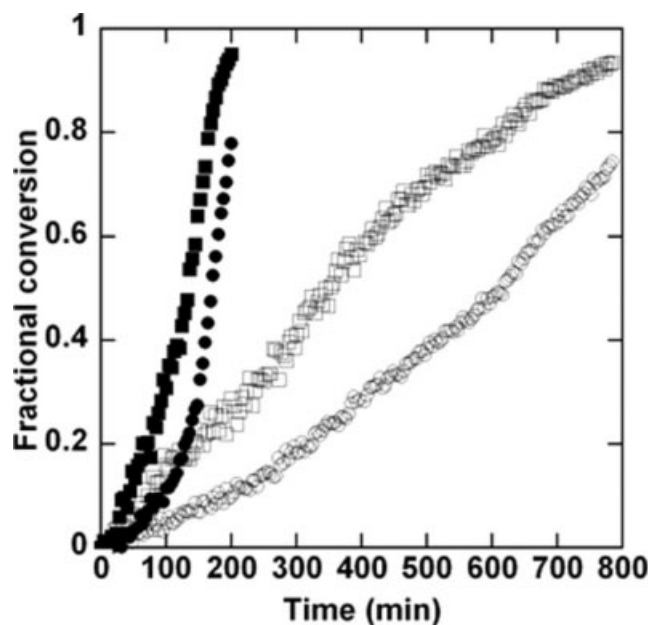

Figure 7 Temporal conversion profiles at 0.002 mol % BPO (open markers) and 0.02 mol % BPO (filled markers) at a VE : AMPS molar ratio of 1 : 2 and 80 wt % solvent content for (□, ■) VE and (○, ●) AMPS.
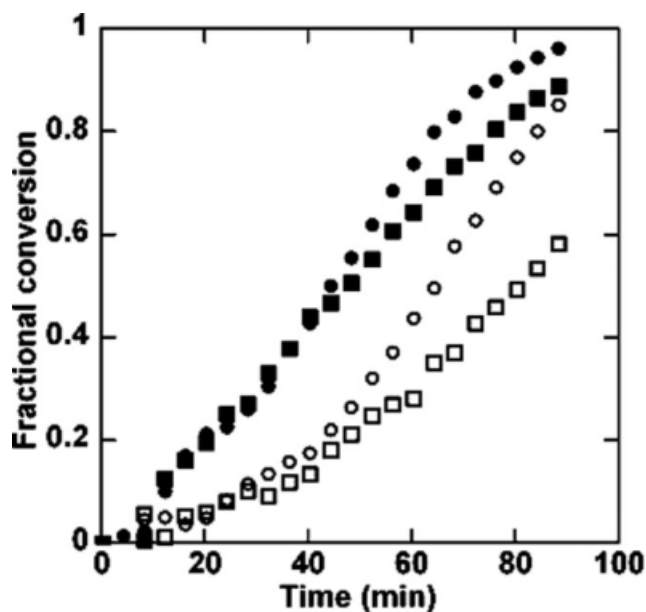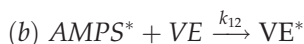
Figure 8 Temporal profiles of fractional conversion for a fixed molar ratio of VE (open markers) to AMPS (filled markers) of 1 : 2 at solvent fractions of ($\bigcirc$, $\bullet$) 71.5 wt % and ($\square$, $\blacksquare$) 80 wt % showing the Trommsdorf effect.

both the reactivity and mechanical characteristics may be studied, VE : AMPS molar ratios of 2 : 1, 1 : 1, 2 : 3, or 1 : 2 were selected.

Significant differences in reactivity when changing the comonomer ratio were observed. Temporal conversion profiles at VE : AMPS comonomer molar ratios of 1 : 1, 2 : 3, and 1 : 2, and solvent content of 75 wt % are given in Figure 9. The plot indicates that increasing the proportion of AMPS increases the rates of conversion in both the VE and AMPS double bonds, similar to findings by others.[41] Higher fractions of AMPS result in a tendency for VE double bonds to react more rapidly. This suggests an increased affinity of activated AMPS moieties for VE monomers. Such behavior is further elucidated by an analysis of the relative reactivity between the AMPS and VE moieties. An understanding of the monomer reactivity ratios sheds light upon the relation between reactivity and structure in radical polymerization reactions. The copolymer composition equation, developed and used extensively elsewhere,[13,21,30] was used as the basis for determining the reactivity ratios. For the VE-AMPS system, the four propagation equations are written as

$$(a) \ \mathrm{AMPS}^* + \mathrm{AMPS} \xrightarrow{k_{11}} \mathrm{AMPS}^*$$

$$(b) \ AMPS^* + VE \xrightarrow{k_{12}} VE^*$$

$$(c) \ \mathrm{VE}^* + \mathrm{AMPS} \xrightarrow{k_{21}} \mathrm{AMPS}^*$$

$$(d) \ \mathrm{VE}^* + \mathrm{VE} \xrightarrow{k_{22}} \mathrm{VE}^*$$

k_{ij} represents the rate constant while the asterisk (*) represents an active chain end. The reactivity ratios for this copolymer system is defined as,

$$r_{\mathrm{AMPS}} = \frac{k_{11}}{k_{12}}; \quad _{\mathrm{VE}} = \frac{k_{22}}{k_{21}}$$

and are a measure of the relative rates of homopolymerization versus copolymerization in a system. The values for r were obtained for conversions below 15%. These are not truly a measure of intrinsic kinetic behavior since the monomer concentration
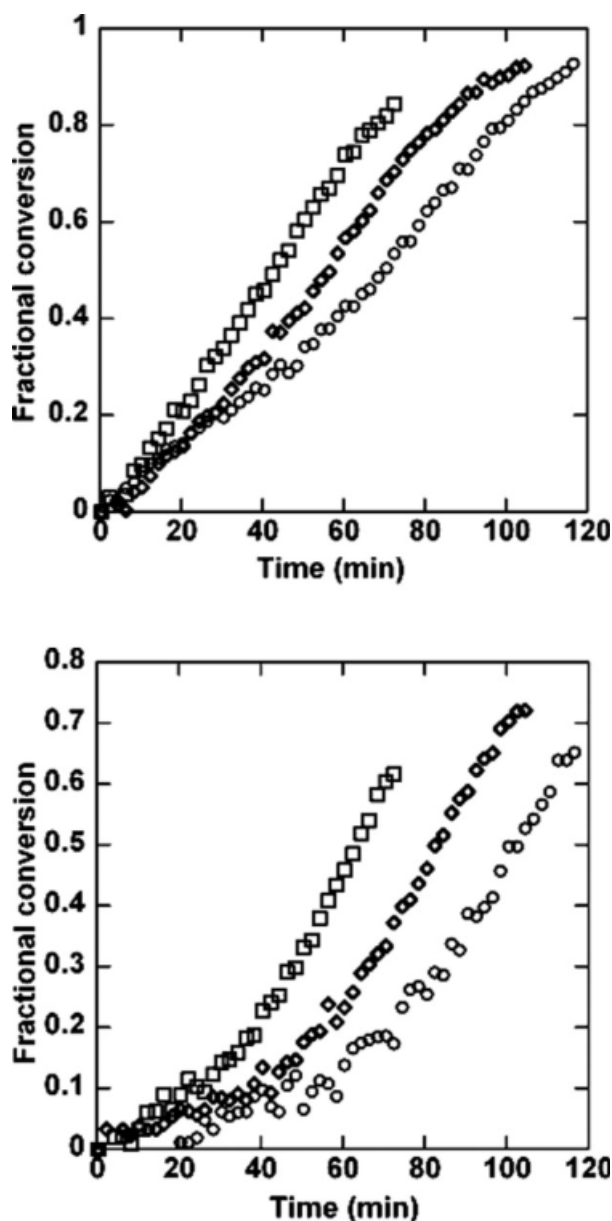

Figure 9 Plots of fractional conversions as a function of time for (*top*) VE and (*bottom*) AMPS at 75 wt % solvent fraction and molar ratios of VE to AMPS of ($\square$) 1 : 2, ($\diamondsuit$) 2 : 3, and ($\bigcirc$) 1 : 1.
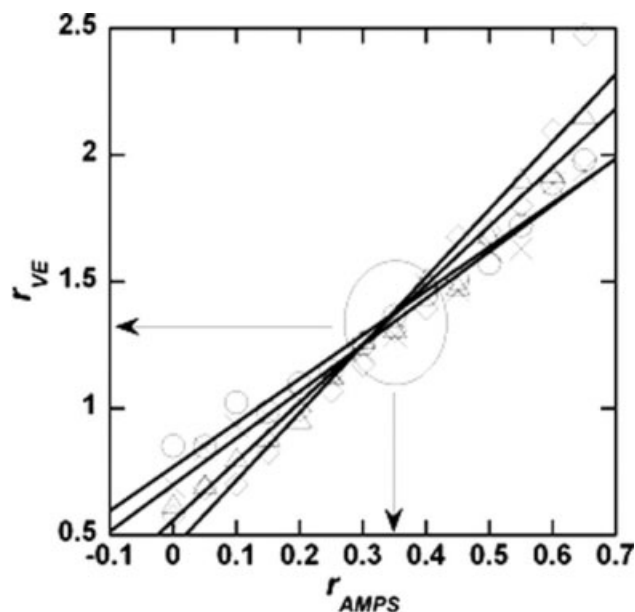
Figure 10 Reactivity ratios of AMPS (r_{AMPS}) and VE (r_{VE}) determined by the Mayo-Lewis method. Plot shows representative data with lines of best fit at VE : AMPS ratios of [(⊖), (✕)] 2 : 1 and [(◇), (△)] 1 : 2, and solvent fractions of [(⊖), (◇)] 75 wt % and [(✕), (△)] and 66.7 wt %. Intersection of lines gives the optimal values of r_{AMPS} and r_{VE}.

and extent of reaction is high.[21] Nevertheless, the results are instructive in the study of thermosets as they provide direct information of what is occurring in the early stages of polymerization. Furthermore, the early stage development of network structure has been found to influence ultimate network structure since gelation occurs at relatively low conversion in these systems, setting network and morphological structure early in the cure process. On the basis of the copolymer equation values of r_{AMPS} and r_{VE} were generated and plotted as shown in Figure 10 for a sample set that spans two different copolymer compositions (at VE : AMPS ratios of 2 : 1 and 1 : 2) and two different solvent contents (66.7 wt % and 75 wt %). The optimum values were determined to be $r_{VE} = 1.35 \pm 0.1$ and $r_{AMPS} = 0.35 \pm 0.1$. These were taken as the x and y values at the intersection of the lines of best fit, and the standard deviations were taken as the breadth of the region of intersection.

From these values of reactivity ratios as well as thermomechanical analyses in the following section, it is evident that significant copolymerization of both monomers is occurring; the absence of which might otherwise lead to "blocky" diphasic or interpenetrating types of networks structures and an overall heterogenous monomer distribution. The value of r_{VE} being close to 1 suggests that the rate of homopolymerization of VE is comparable to the addition of a reactive AMPS unit onto a VE. On the other hand,

since r_{AMPS} is less than 1, this suggests that the copolymerization of AMPS with reactive VE units is favored more than the homopolymerization between AMPS moieties. The product of r_{VE} and r_{AMPS} gives information about the overall copolymer structure in between being an ideal random structure ($r_{VE}.r_{AMPS} \sim 1$) or alternating ($r_{VE}.r_{AMPS} \sim 0$).[13,32] Since the product between r_{VE} and r_{AMPS} lies between this range with a value close to 0.5, the overall copolymer structure is expected to be a moderately random arrangement of VE and AMPS in the composition range investigated. Also, since $r_{VE} > 1$ while $r_{AMPS} < 1$, it is expected that at initial times, there is a faster consumption of VE (through both homopolymerization and copolymerization) as compared with AMPS. This reflects the higher reaction rates of VE as compared with AMPS discussed in previous sections.

The occurrence of a random dispersion of AMPS within a network structure is desirable for applications where the requirement is to obtain sufficient ionic conductivity which in turn depends on the connectivity between sulfonic acid groups on AMPS moieties. The reason for this is that although the development of VE network structure provides greater mechanical stability, the mobility required for large scale ionic aggregate formation through rearrangement after complete cure which occurs in linear polymers is curtailed in crosslinked structures. The investigation of proton conductivity in these materials is the subject of a separate communication.[42]
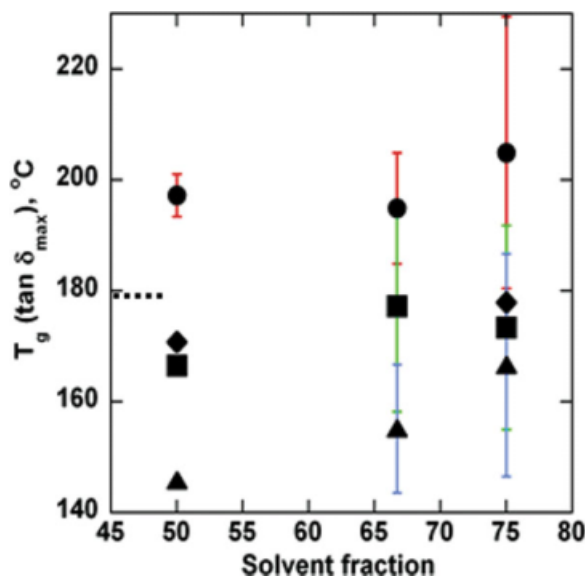

Figure 11 Variation in T_g with solvent content at differing comonomer feed ratios and solvent contents; supercritically dried samples at VE:AMPS comonomer ratios of (■) 0, (●) 2 : 1, (◆) 1 : 1 and (▲) 1 : 2 and (- - -) VE without supercritical extraction. [Color figure can be viewed in the online issue, which is available at www.interscience.wiley.com.]

Thermomechanical behavior and solvent effects on network structure

Dynamic mechanical tests were used to connect comonomer reactivities to mechanical behavior. Figure 11 shows the values of the glass transition temperature, T_g, taken as the tan δ maximum for copolymers at VE : AMPS molar ratios of 2 : 1, 1 : 1, and 1 : 2 dried using supercritical carbon dioxide. The plot also shows the T_g for supercritically dried VE homopolymers at different solvent fractions and pure VE. At molar ratios of 1 : 1 and 1 : 2, the T_g's are lower than that of the homopolymers at comparable solvent fractions. This is probably due to the plasticizing effect that AMPS has on a highly crosslinked VE network and is similar to trends observed previously in VE-styrene systems,[43] where a higher styrene content results in lowered T_g's. At a VE : AMPS ratio of 2 : 1 though, the T_g's are higher than those of the VE homopolymers. It suggests that low AMPS concentrations might cause previously inaccessible vinyl groups to further react into the network. This could result in the reduced formation of microgels which are known to occur in VE networks,[21] that could otherwise potentially lower the T_g by trapping unreacted chain ends.

An increase in the solvent fraction at constant comonomer ratios does not cause appreciable declines in T_g that might be expected due to cyclization.[44–46] Rather, Figure 11 shows a generally constant or slightly increasing trend in the T_g of the VE homopolymer and the copolymers. Table II compares the T_g's of the thermally and supercritically dried out films at two comonomer ratios and different solvent fractions. The increase in the T_g of the copolymers with increased solvent fractions occurs irrespective of drying technique. The observed increase in T_g is probably due to a higher ultimate conversion at high solvent fractions,[47] as the T_g of a polymer is known to be proportional to the conversion. The increased T_g does not appear to be explainable in any other way, since the presence of residual solvent or cyclization, would lead to a decrease in
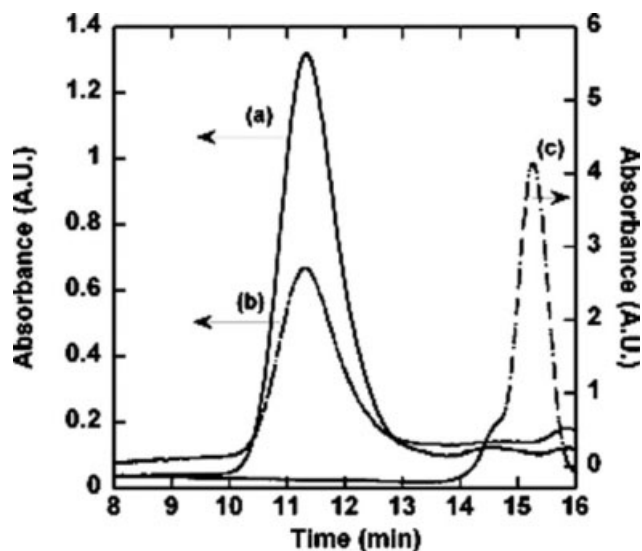

Figure 12 Representative GPC traces of liquid phase extract showing unbound, high molecular weight, and unreacted lower molecular weight fractions from samples that are (a) thermally dried versus (b) supercritically dried at a VE : AMPS ratios of 1 : 1 and a 75 wt % solvent fraction compared with (c) pure VE.

T_g. Although Figure 2 shows an apparent completion of the reaction, it is known that IR instrumentation is not sensitive to within a few percent[48] and this could be an explanation for the absence of measurable reaction at very high degrees of conversion.

From Table II, the measured T_g's of the supercritically dried samples are higher than the thermally dried samples. This suggests that the presence of any residual solvent may not be the primary reason for the depressed T_g in thermally dried samples but is rather due to the presence of some other fraction that softens the thermoset. Figure 12 shows GPC traces comparing the soluble extract from thermally and supercritically dried copolymers at a 75 wt % solvent fraction and a 1 : 1 molar ratio of VE to AMPS. The GPC trace of pure VE is also shown for comparison. The plot suggests a small fraction of an extractable phase with a retention time of 11.5 minutes ($M_w = 32{,}000$, based on polystyrene standards) and corresponds to molecules that are not covalently bound to the crosslinked network. Although these molecules show up in both the thermally and supercritically dried samples, it occurs at a relatively lower concentration in the latter. This implies that the fraction of chains not contributing to overall network formation is being extracted with the aid of the CO_2 used during the drying process. The extraction does not take place during thermal drying as only the DMF may be vaporized during temperature ramps. It is possible that it is this increased fraction of unbound molecules in thermally dried samples which contributes toward a net lowered T_g.

TABLE II
Comparison Between Thermally Dried and Supercritically Dried Films at Varying Solvent Contents and Molar AMPS Concentration

Solvent content (%)	67% (Thermal) (°C)	67% (Scdried) (°C)	50% (Thermal) (°C)	50% (Scdried) (°C)
50	124	146	126	167
66.7	121	147	a	164
75	128	152	141	160
80	135	a	152	a
83.3	139	a	a	a

[a] Not measured.

SUMMARY

The results of this work show that it is possible to realize a combination of hydrophobic and hydrophilic, well-dispersed, and mechanically stable copolymers via a thermally initiated, free radical copolymerization scheme. The method developed to track the methacrylate-acrylate reaction was found to be useful in studying polymerization kinetics. The analysis developed can be used to study the kinetics of similar copolymerizing methacrylate-acrylate type systems. The computed reactivity ratios indicates a random copolymer structure being formed for the investigated comonomer ratios while thermo-mechanical analysis indicates a minimum glass transition temperature of 121°C in a solvent-free membrane. Increasing solvent fractions causes an increase in the T_g and is suggested to be due to increased ultimate conversions. Comparisons between drying techniques indicated a small fraction of a high-molecular weight, soluble phase within the network that lowered the glass transition temperature. Ongoing work on the analysis of proton conductivity and water uptake behavior will shed light on the properties that make these membranes interesting in electrochemical applications.

References

1. Osada, Y.; Gong, J. P. Adv Mat 1998, 10, 827.
2. Maruyama, Y.; Ishii, T.; Suzuki, A. J Appl Phys 1996, 80, 131.
3. Karlsson, L. E.; Wesslen, B.; Jannasach, P. Elec Acta 2002, 47, 3269.
4. Elabd, Y. A.; Napadensky, E.; Sloan, J. M.; Crawford, D. M.; Walker, C. W. J Membr Sci 2003, 217, 227.
5. Snedden, P.; Cooper, A. I.; Scott, K.; Winterton, N. Macromolecules 2003, 36, 4549.
6. Kapur, V.; Charkoudian, J. C.; Kessler, S. B.; Anderson, J. L. Ind Eng Chem Res 1996, 35, 3179.
7. Dessouki, A. M.; Taher, N. H.; El-Arnaouty, M.; Khalil, F. H. J Appl Poly Sci 1993, 48, 1249.
8. Robinette, E. J.; Palmese, G. R. Nucl Instr Meth Phys Res B 2005, 236, 216.
9. Hong, L.; Chen, N. J Poly Sci B: Poly Phys 2000, 38, 1530.
10. Bo, Z.; Rabe, J. P.; Schlüter, A. D. Ang Chemie Int Ed 1999, 38, 2370.
11. Webster, O. W. Science 1991, 251, 887.
12. Baines, F. L.; Billingham, N. C.; Armes, S. P. Macromolecules 1996, 29, 3416.
13. Odian, G. Principles of Polymerization; John Wiley and Sons, Inc.: Hoboken, New Jersey, 2004.
14. Allcock, H. R.; Lampe, F. W. Contemporary Polymer Chemistry; Prentice Hall, 1981.
15. Akashi, M.; Yanagi, T.; Yashima, E.; Miyauchi, N. J Polym Sci Part A: Poly Chem 1989, 27, 3521.
16. Okano, T.; Katayama, M.; Shinohara, I. J Appl Poly Sci 1978, 22, 369.
17. Pei, H.; Hong, L.; Lee, J. Y. J Power Sources 2006, 160, 949.
18. Cho, K. Y.; Jung, H. Y.; Shin, S. S.; Choi, N. S.; Sung, S. J.; Park, J. K.; Choi, J. H.; Park, K. W.; Sung, Y. E. Elec Acta 2004, 50, 588.
19. Won, J.; Park, H. H.; Kim, Y. J.; Choi, S. W.; Ha, H. Y.; Oh, I.-H.; Kim, H. S.; Kang, Y. S.; Ihn, K. J. Macromolecules 2003, 36, 3228.
20. Walker, C. W. J Power Sources 2002, 110, 144.
21. Ziaee, S.; Palmese, G. R. J Poly Sci Part B: Poly Phys 1999, 37, 725.
22. Scott, T. F.; Cook, W. D.; Forsythe, J. S. Polymer 2002, 43, 5839.
23. Gramm, S.; Komber, H.; Schmaljohann, D. J Poly Sci Part A: Poly Chem 2005, 43, 142.
24. Paczkowski, J.; Neckers, D. C. Macromolecules 1992, 25, 548.
25. Rey, L.; Galy, J.; Sautereau, H.; Lachenal, G.; Henry, D.; Vial, J. Appl Spectrosc 2000, 54, 39.
26. Stansbury, J. W.; Dickens, S. H. Dental Mater 2001, 17, 71.
27. Lousberg, H. H. A.; Boelens, H. F. M.; Le Comte, E. P.; Hoefsloot, H. C. J.; Smilde, A. K. J Appl Poly Sci 2002, 84, 90.
28. Long, T. E.; Liu, H. Y.; Schell, B. A.; Teegarden, D. M.; Uerz, D. S. Macromolecules 1993, 26, 6237.
29. Beyers, C. P.; Boelens, H. F. M.; Klumperman, L.; Westerhuis, J. A. Appl Spectr 2004, 58, 863.
30. Mayo, F. R.; Lewis, F. M. J Am Chem Soc 1944, 66, 1594.
31. Robinette, E. J.; Ziaee, S.; Palmese, G. R. Polymer 2004, 45, 6143.
32. Pasquale, A. J.; Long, T. E. J Appl Poly Sci 2004, 92, 3240.
33. Wiles, K. B.; Bhanu, V. A.; Pasquale, A. J.; Long, T. E.; McGrath, J. E. J Poly Sci Part A: Poly Chem 2004, 42, 2994.
34. Raman, V. I.; Palmese, G. R. Colloids Surf A 2004, 241, 119.
35. La Scala, J. J.; Sands, J. M.; Orlicki, J. A.; Robinette, E. J.; Palmese, G. R. Polymer 2004, 45, 7729.
36. Raman, V. I.; Palmese, G. R. Macromolecules 2005, 38, 6923.
37. Ingle, J. D. C.; Stanley R. Sprectrochemical Analysis; Prentice Hall: New Jersey, 1988.
38. Elliott, J. E.; Anseth, J. W.; Bowman, C. N. Chem Eng Sci 2001, 56, 3173.
39. O'Neil, G. A.; Wisnudel, M. B.; Torkelson, J. M. Macromolecules 1998, 31, 4537.
40. Brill, R. P.; Palmese, G. R. J Appl Poly Sci 2000, 76, 1572.
41. Zhang, C.; Easteal, A. J. J Appl Poly Sci 2003, 88, 2563.
42. Rahmathullah, M. A.; Snyder, J.; Elabd, Y. A.; Palmese, G. R. submitted.
43. Auad, M. L.; Aranguren, M. I.; Borrajo, J. J Appl Poly Sci 1997, 66, 1059.
44. Okay, O.; Kurz, M.; Lutz, K.; Funke, W. Macromolecules 1995, 28, 2728.
45. Elliott, J. E.; Bowman, C. N. Macromolecules 2002, 35, 7125.
46. Elliott, J. E.; Nie, J.; Bowman, C. N. Polymer 2003, 44, 327.
47. Hale, A.; Macosko, C. W.; Bair, H. E. Macromolecules 1991, 24, 2610.
48. Ganem, M.; Lafontaine, E.; Mortaigne, B.; Bellenger, V.; Verdu, J. J Macro Sci 1994, B33, 155.